Biophysical Chemistry 6 (1977) 201–211

MOLECULAR DYNAMICS THROUGH ^2H SPIN-LATTICE RELAXATION TIME MEASUREMENTS WITHIN AN ENZYME-INHIBITOR COMPLEX: LYSOZYME AND METHYL N-ACETYL GLUCOSAMINIDES

László SZILÁGYI
Department of Organic Chemistry, L. Kossuth University, H-4010 Debrecen, Hungary

János HARANGI
Department of Biochemistry, L. Kossuth University, H-4010 Debrecen, Hungary

and

Lajos RADICS
NMR Laboratory, Central Research Insitute for Chemistry of the Hungarian Academy of Sciences, 1525 Budapest, pf. 17, Hungary

Received 24 June 1976

Deuteron spin-lattice relaxation times of specifically labelled methyl N-acetyl-D-glucosaminides associated to lysozyme were measured from ^1H and ^2H NMR spectra through bandshape analysis and FT inversion-recovery technique, respectively. Model calculations were carried out in order to assess the limits of the extreme narrowing approximation for the systems studied. Rotational correlation times of the acetamido methyl groups were analyzed in terms of anisotropic overall reorientation combined with internal rotation. The acetamido methyl group undergoes fast internal rotation in the α-glycoside complex about an axis nearly parallel with the major ellipsoidal axis of lysozyme. More rotational freedom is likely to occur in the β-glycoside complex.

1. Introduction

Detailed structural information is available nowadays for many enzymes through X-ray crystallographic studies. This is not the case for enzyme-substrate complexes whose molecular topography is generally not accessible to direct experimental observation on account of the short lifetime and low concentration of these complexes. This difficulty may be circumvented to some extent by using substrate-like, or inhibitor, molecules that form stable complexes with the enzyme. One of the best examples was given by D.C. Phillips' group [1,2] through X-ray determination of the three-dimensional structure of stable complexes of lysozyme with the inhibitors N-acetyl-D-glucosamine (NAcGlc) and its β(1→4) trimer. It was this structure determination that provided a sound basis for theories aimed at explaining the mechanism of the glycoside cleaving reaction catalyzed by lysozyme [3–5].

Reactions catalyzed by soluble enzymes, like lysozyme, take place, however, in solution. Therefore, it is reasonable to assume that, in addition to the static structural information obtained through X-ray crystallography, a knowledge of the dynamic molecular topography of the enzyme-inhibitor (EI) complexes in solution would be of great importance for rationalizing molecular events that occur during an enzyme-catalyzed reaction.

NMR spectroscopy has been shown to furnish useful structural and dynamical information in the liquid state which permit to gain some insight into both aspects of the enzyme-inhibitor (or, possibly, the enzyme-substrate) interaction. Of special interest, in this respect, is the relaxation of deuterium nuclei, and mainly for two reasons: (i) relaxation of ^2H is almost exclusively dominated by the quadrupolar mechanism and (ii) only *intramolecular* motions contribute to the relaxation process. This is not the case, for instance, with proton relaxation since, generally, both intra-

and intermolecular interactions as well as more than one relaxation mechanism may contribute to the measured relaxation time. The advantages of using ^2H relaxation for studying molecular reorientations have been extensively discussed [6]. It is to be noted that, for investigating the molecular motions of a species participating in a chemical equilibrium, it is essential to have a unique relaxation mechanism since the separation of various contributions to the observed relaxation time cannot, in general, be done (by changing the concentration or temperature, for instance) without disturbing the equilibrium.

As a first step towards studying the molecular dynamics of a small molecule bound to the active site of an enzyme we set out to investigate the interactions between lysozyme and the inhibitors, methyl α- and β-N-acetyl-D-glucosaminides (Me α- and β-NAcGlc). It is well known [7,8] that lysozyme binds these monosaccharides specifically at subsite C of the active site. Apparent association constants [9] and kinetic data [10] characterizing this association process were determined by NMR spectroscopy. It was also shown [11] through the charge transfer interaction between the Trp-62 residue of lysozyme and an electron acceptor group attached to Me α-NAcGlc that this complex is similar in structure to that of monosaccharide inhibitors in solution (as determined by NMR) on the one hand, and in the crystalline state (X-ray analysis), on the other. Thus, the structures of EI complexes of lysozyme with monosaccharide inhibitors are fairly well known and sufficient evidence exists to indicate that the solution structures are similar to those determined by X-ray analysis in the crystalline state.

On the basis of this knowledge it was our purpose to investigate the applicability of the ^2H spin-lattice relaxation approach to molecular dynamics of EI complexes using the well-known system lysozyme – methyl 2-acetamido-2-deoxy-D-glucopyranosides.

The N-acetyl group plays an essential role in binding of these glycosidic inhibitors to lysozyme. It was shown [12] that more than half of the total free energy of association between lysozyme and NAcGlc can be accounted for by the interaction of the enzyme with the N-acetyl group. This is in agreement with the crystallographic result [1,2] showing that the N-acetyl group is involved in two hydrogen bonds out of the four that "tie" the NAcGlc molecule to subsite C. Therefore, the N-acetyl methyl group was selected to obtain rotational correlation times characteristic of the molecular motion of the EI complexes of lysozyme with Me α- and β-NAcGlc. These correlation times were obtained by measuring the spin-lattice relaxation times of deuterons built into the N-acetyl methyl group of these inhibitors. Following labelled compounds were used: Me α-NAc-d_1-Glc (1), Me β-NAc-d_1-Glc (2), Me α-NAc-d_3-Glc (3) and Me β-NAc-d_3-Glc (4).

Measurement of the relaxation time at *one* specific site of the inhibitor molecule conveys motional information only about that part of the molecule where the label (^2H nucleus) had been attached (in our case the NAc methyl group). In order to obtain a complete motional picture *multiply labelled* inhibitors should be used. Such studies are now in progress in our laboratories.

2. Methods

2.1. Measurement of ^2H spin-lattice relaxation times

^2H spin-lattice relaxation times [$T_1(^2H)$] can be measured either via direct observation of ^2H resonance (mostly by pulsed FT methods [e.g. 13]) or indirectly, through bandshape analysis of the proton(s) spin- coupled to the ^2H nucleus under study. The latter method was developed and extensively used by Lehn and coworkers [6]. Also, its merits and drawbacks were thoroughly discussed in ref. [6].

Because of its significantly less instrument time requirement, in this work, the latter experimental approach was generally used. An iterative least squares program was written for extracting $T_1(^2H)$ values from the proton bandshape of the CH_2D–CO group. The bandshape equation given by Kintzinger et al. [14] was used in the fitting procedure i.e. the apparent proton spin-spin relaxation time, $T_2^*(^1H)$, was included into the diagonal elements of the bandshape matrix [15]. It was found that it is essential to have a good proton T_2^* value in order to get reliable values for the ^2H spin-lattice relaxation times since an equally good fit could be obtained for a different $T_1(^2H)$ using $T_2^*(^1H)$ different from the right one. $T_2^*(^1H)$ values were therefore obtained in separate experiments (section 4.1) and fed into the bandshape program as input data. Occasionally, $T_1(^2H)$'s were also measur-

ed by the direct method using the standard inversion-recovery FT technique [16].

2.2. Effects of chemical exchange on the relaxation behaviour

If molecule I containing the relaxation vector (in our case the C-D bond) undergoes chemical exchange between "free" and "bound" environments according to the simple scheme,

$$E + I \underset{k_4}{\overset{k_3}{\rightleftharpoons}} EI,$$

the spin-lattice relaxation time of a given nucleus in molecule I will depend on the rate constants k_1, k_2, k_3 and k_4, where k_1 and k_2 are the rotational rate constants of the relaxation vector in the "free" (I) and "bound" (EI) state, respectively.

The problem of coupling the relaxation phenomena and chemical exchange has been treated by several authors (for references, see [17]). Here we use the formulae given by Anderson and Fryer [18] which are pertinent to our case. The observed relaxation rate, $(T_{1\,obs})^{-1}$, in the extreme narrowing limit, is

$$(T_{1\,obs})^{-1} = B(Q_+/\lambda_+ + Q_-/\lambda_-), \tag{1}$$

where

$$\lambda_\pm = \tfrac{1}{2}(k_1 + k_2 + k_3F + k_4) \pm \tfrac{1}{2}[(k_1 + k_3F - k_2 - k_4)^2 + k_3k_4F]^{1/2},$$

$$Q_+ = \frac{k_+ - 1}{k_+ - k_-}[1 - (1 - k_-)C], \tag{2}$$

$$Q_- = \frac{1 - k_-}{k_+ - k_-}[1 - (1 - k_+)C],$$

with $k_\pm = k_4/(\lambda_\pm - k_1 - k_3F)$ and $C = [EI]/[I_0]$ the complexed fraction of I, $F = [E_0] - C[I_0]$ the concentration of the free E molecules. $[E_0]$ and $[I_0]$ denote initial analytical concentrations.

For quadrupolar relaxation the interaction constant B is equal to $\frac{3}{8}(e^2qQ/\hbar)^2$. It has been shown [18] that in the limiting case when k_3, $k_4 \ll k_1$, k_2,

$$(T_{1\,obs})^{-1} = CB/k_2 + (1 - C)B/k_1 = C(T_{1c})^{-1} + (1 - C)(T_{1f})^{-1}, \tag{3}$$

where T_{1f} and T_{1c} are the relaxation times in the free and complexed environments, respectively.

Outside the extreme narrowing limit, i.e. when the inequality $\lambda_+, \lambda_- \gg \omega_0$ does not hold, $T_{1\,obs}$ depends on ω_0 [18]

$$(T_{1\,obs})^{-1} = \frac{B}{5}\left[\frac{Q_+/\lambda_+}{1+(\omega_0/\lambda_+)^2} + \frac{4Q_+/\lambda_+}{1+4(\omega_0/\lambda_+)^2} + \frac{Q_-/\lambda_-}{1+(\omega_0/\lambda_-)^2} + \frac{4Q_-/\lambda_-}{1+4(\omega_0/\lambda_-)^2}\right], \tag{4}$$

where ω_0 is the Larmor frequency in rad s^{-1} of the nucleus under study.

3. Experimental procedures

3.1. Deuterated compounds

bis(Acetic-d_1)anhydride was prepared [19] from ketene by bubbling it through deuterium oxide (Merck, UVASOL, 99.75% isotopic purity).

Methyl α- and β-N-acetyl-d_1-2-amino-2-deoxy-D-glucopyranosides (Me α- and β-NAc-d_1-Glc), 1 and 2. Glucosamine·HCl was selectively N-acetylated [20] with bis(acetic-d_1)anhydride and the resulting N-acetyl-d_1-2-deoxy-2-amino-α-D-glucopyranose was treated [21] with methanol in the presence of a cation exchange resin, BIO-RAD AG-50W-8X (H^+-form). The mixture of the anomeric methyl glycosides, 1 and 2, was separated [21] on a charcoal-Celite column using water-ethanol as eluant. Alternatively, the β-anomer, 2, was also prepared [22] through Koenigs-Knorr reaction from N-acetyl-d_1-3,4,6-tri-O-acetyl-2-amino-2-deoxy-α-D-glucopyranosyl chloride [20] and methanol, followed by O-deacetylation with sodium methoxide in methanol.

Methyl α- and β-N-acetyl-d_3-2-amino-2-deoxy-D-glucopyranosides (Me α- and β-NAc-d_3-Glc), 3 and 4. These compounds were prepared in the same manner as described for 1 and 2 using acetic-d_6 anhydride (Merck, 98% isotopic purity).

3.2. Preparation of the samples

Lysozyme, twice crystallized and salt-free, was obtained from Worthington (code LYSF) and used without any further treatment for the direct $T_1(^2H)$ deter-

mination. For T_1 measurements by the bandshape method, a 10% solution of lysozyme in water was dialyzed against 10^{-3} mol dm^{-3} acetic-d_4 acid in water for 48 hours at 2–5° to remove the acetate which was present in the commercial preparation. No acetate could be detected by NMR after this treatment. The dialyzed sample was then lyophilized from deuterium oxide 2–3 times. The enzymatic activity was checked before and after each series of measurements by spectrophotometric determination [23] of the rate of lysis of *Micrococcus Lysodeikticus* cells (Worthington). No significant change of enzymatic activity occurred during measurements. Enzyme concentrations were determined from the UV absorbance at 280 nm using a molar absorbance coefficient [24] $\epsilon_M = 3.6 \times 10^4$ mol^{-1} cm^{-1}.

Since it is known [24] that ionic strengths higher than 0.08 inhibit the enzymatic activity of lysozyme, all relaxation time measurements were carried out at pH = 6.0 in 0.066 mol dm^{-3} phosphate buffer (ionic strength 0.08). D_2O and H_2O were used for the ^1H and ^2H measurements, respectively. The pH values refer to direct meter readings. Stock inhibitor solutions (2×10^{-2} mol dm^{-3} and 4×10^{-2} mol dm^{-3} for ^1H and ^2H work, respectively) were prepared with the above buffers, and a starting enzyme-inhibitor solution was obtained by adding an amount of lysozyme to an aliquot of the stock solution so as to get a complexed mole fraction, $C = [EI]/[I_0]$, of about 0.08–0.1 for the inhibitor. C is easily calculated on the basis of the simple equilibrium, $E + I \rightleftharpoons EI$. If the apparent association constant, $K = [EI]/[E][I]$, is known,

$$C = \{K([E_0] + [I_0]) + 1 - \{[K([E_0] + [I_0]) + 1]^2 - 4[E_0][I_0]K^2\}^{1/2}\}/2[I_0]K,$$

where $[E_0]$ and $[I_0]$ denote the analytical concentrations in mol dm^{-3} of the enzyme and the inhibitor, respectively. This calculation was included into the program RCT (vide infra). The starting solution was then diluted with the stock inhibitor solution so that the complexed fraction was gradually decreased while the inhibitor concentration remained constant.

3.3. NMR measurements

A Varian XL-100/15 NMR instrument, equipped with Varian S 124X FT accessory and a 620L 16K computer, was used. For bandshape analysis, the CH_2D proton triplet was recorded in c.w. mode, using 50 Hz sweep widths and 0.05 Hz s^{-1} sweep rate. The spectra were manually "smoothed" and digitized by taking the signal amplitudes at every 0.1 Hz. Only the right half of the triplet was considered; the left part being distorted by the presence of the residual methyl resonance (cf. ref. [14]). Up to 30–35 data points were used in the calculation of the ^2H spin-lattice relaxation times.

Direct $T_1(^2H)$ determinations were carried out at 15.36 MHz employing the standard FT inversion-recovery technique [16]. The accuracy was checked by reproducing published [25] $T_1(^2H)$ value of $CDCl_3$ (measured: 1.45 ± 0.03 s; lit. [25]: 1.47 s ± 4%). For reasons of sensitivity compounds **3** and **4**, containing fully deuterated methyl groups, were used at a concentration of 0.04 mol dm^{-3}.

^{13}C spin-lattice relaxation times, $T_1(^{13}C)$, were measured at 25.16 MHz using the FT inversion-recovery method [16]. NOE values for ^{13}C nuclei were obtained by gated ^1H noise decoupling and subsequent integration of individual resonances. The accuracy of $T_1(^{13}C)$ measurements is estimated to be of 5–10% and that of NOE values 10%.

All measurements were done at ordinary probe temperature of 30 ± 1° using 12 mm o.d. sample tubes.

3.4. Data analysis

The bandshape analysis was performed essentially in the manner described in ref. [14]. A program (QRT) was written in ALGOL for an ODRA 1204 computer. This was a modified version of the original program by Kintzinger [26]. Input data were the digitized experimental spectra. $T_1(^2H)$, $T_2^*(^1H)$ and $J_{H,D}$, the proton-deuteron spin–spin coupling constant, may be iterated to obtain a least squares fit between experimental and computed spectra. However, for reasons mentioned in section 2.1, $T_2^*(^1H)$ values were determined from the CH_3–CO proton line widths of Me α-NAcGlc and fed into the program as input data. The error in $T_1(^2H)$ data obtained in this way is generally less than 10% and typically is around 5% (see table 2).

The $T_1(^2H)$ values were fitted to eqs. (1) and (4) using an iterative program (RCT) in which all of the

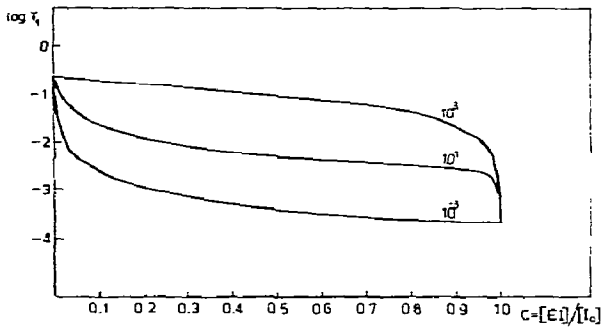

Fig. 1. Semilog plot of T_1 versus C for a quadrupolar nucleus of spin 1 in molecule I undergoing rotational relaxation and chemical exchange. Following constants were used in eq. (1) $B = 4.3 \times 10^{11}\ s^{-2}$ (quadrupolar coupling constant 170 kHz), $k_1/k_2 = 10^3$, $k_3/k_4 = 1$. The number next to each curve gives the ratio k_4/k_2.

rate constants, k_1, k_2, k_3 and k_4 could be iterated. However, with k_3 and k_4 as well as k_1 being known from independent measurements (section 4.1) the number of unknown parameters was reduced to one (k_2) which greatly improved the reliability of the calculated k_2 value. Output of the program was the value of $k_2 = \tau_{compl}^{-1}$ and T_{1c} (see section 4.1).

4. Results and discussion

4.1. Determination of T_{1c} and k_2

In order to obtain motional information about molecule I in the EI state we have to know the spin-lattice relaxation times in *this* environment (T_{1c}). In view of the rapid equilibrium and, associated with it, the low concentration of the EI species, T_{1c} is inaccessible to direct measurements. Its value can, however, be derived by extrapolating $T_{1\,obs}$ to the limit $C = 1$. Two problems emerge at this point: (i) the rate constants k_1, k_2, k_3 and k_4 must be known; (ii) decision must be made as to whether eq. (1) or (4) is the correct one to be used in the extrapolation procedure (in other words, whether or not the extreme narrowing condition is valid for the system under study).

It has been shown [18] that plots of $T_{1\,obs}$ versus C yield characteristic curves for different k_4/k_2 ratios. Calculated curves (using eq. (1)) for a quadrupolar nucleus in molecule I are shown in fig. 1. As it can be

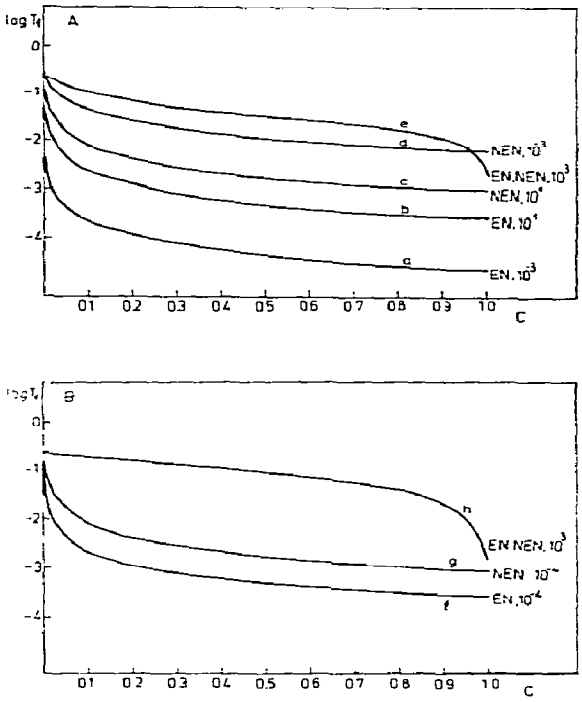

Fig. 2. Semilog plot of T_1 versus C for a quadrupolar nucleus of spin 1 calculated from eq. (1) (extreme narrowing case, EN) and eq. (4) (non-extreme narrowing case, NEN). Constants used are $B = 4.3 \times 10^{11}\ s^{-2}$, $\omega_0 = 10^8$ rad s^{-1} (the approximate Larmor frequency of the ^2H nucleus in a 2.35 T magnetic field). $k_1 = 10^{11}\ s^{-1}$, $k_2 = 10^7\ s^{-1}$ (A); $k_1 = 10^{11}\ s^{-1}$, $k_2 = 10^8\ s^{-1}$ (B). The number next to each curve gives the ratio k_4/k_2.

seen, for small values of k_4/k_2 (i.e., when dissociation of the EI complex is slow with respect to its reorientation rate) $T_{1\,obs}$ decreases rapidly with increasing complexed mole fraction. Numerical evaluation of $T_{1\,obs}$ versus C using eq. (4) gives, for small k_4/k_2 ratios, different curves in the extreme narrowing ($\lambda_+, \lambda_- \gg \omega_0$) and the non-extreme narrowing ($\lambda_+, \lambda_- \leqslant \omega_0$) cases (e.g. curves a and d in fig. 2). This difference diminishes, as expected, on approaching the extreme narrowing limit (compare curves f and g). On the other hand, both eqs. (1) and (4) predict identical relaxation behaviour when $k_4/k_2 \gg 1$ (curves e and h). It is clear therefore that, studying $T_{1\,obs}$ as a function of C, the extreme narrowing and non-extreme narrowing cases can only be distinguished when "true" complex for-

Table 1
Association and rate constants for lysozyme –Me α- and β-NAcGlc complexes

Constant	Me α-NAcGlc	Me β-NAcGlc	Conditions	Ref.
K_a(mol^{-1})	25.6±3	34.5±4	pH=5.3 no buffer	[10]
	19.2±1.4	30.3±4	pH=5.5 0.1M citrate	[9]
k_3(mol^{-1} s^{-1})	1.4±0.7×10^5	1.6±0.8×10^5	pH=5.3 no buffer	[10]
k_4(s^{-1})	5.5±2.1×10^3	4.5±1.7×10^3	pH=5.3 no buffer	[10]

mation takes place (i.e. when $k_4/k_2 \ll 1$) in the system studied.

In deriving the values of rate constants k_1, k_2, k_3 and k_4 (point (i) above) we may proceed as follows. For a quadrupolar nucleus of spin 1 in molecule 1, $k_1 = \tau_{free}^{-1}$ can be calculated from the relaxation time of this nucleus in the "free" inhibitor, T_{1f}, [15]

$$(T_{1f})^{-1} = \tfrac{3}{8}\,(e^2qQ/\hbar)\,\tau_{free}. \qquad (5)$$

The remaining constants, k_2, k_3 and k_4 may be obtained by fitting $T_{1\,obs}$ as a function of C to eqs. (1) or (4). A similar approach has been used by Brévard and Lehn [27] in a study of molecular dynamics of π–π complex formation. Since the values of k_3 and k_4 for complexes of lysozyme with Me α- and β-NAcGlc are known the number of parameters to be fitted can be reduced to one (k_2). The relevant literature data on the association and rate constants are summarized in table 1.

The results of the ^{2}H spin-lattice relaxation time measurements are shown in table 2. The majority of these data were obtained through bandshape analysis. The $T_2^*(^1H)$ values used in the calculations (section 2.1) were taken from the half-widths ($\Delta\nu_{1/2}$) of the N-acetyl methyl ^{1}H signal measured in α-NAcGlc as a function of the complexed fraction C (fig. 3). Extrapolation to $C=1$ gave $\Delta\nu_{1/2\ complex} \approx 12$Hz for the linewidth of the bound inhibitor in agreement with reported [28] results, $\Delta\nu_{1/2\ complex} \sim 10$–20 Hz. $T_2^*(^1H)$ values obtained from the curve in fig. 3 were used for the β-anomer as well.

Values of $k_1 = \tau_{free}^{-1}$ were calculated with the aid of eq. (5) using $T_1(^2H)$ data for $C=0$ taken from table 2.

Table 2
^{2}H spin-lattice relaxation times for the CH_2D–CO groups in Me α-NAc-d_1-Glc and Me β-NAc-d_1-Glc in the presence of varying amounts of lysozyme

$C=[EI]/[I_0]$	$T_1(^2H)$ (s)	$C=[EI]/[I_0]$	$T_1(^2H)$ (s)
Me α-NAc-d_1-Glc		Me β-NAc-d_1-Glc	
0	0.294±0.014 (5)	0	0.272±0.004 (4)
	0.360[a]		0.360[a]
8.60×10^{-4}	0.274±0.016 (3)	9.74×10^{-4}	0.220±0.017 (2)
2.17×10^{-3}	0.219±0.026[b] (2)	2.43×10^{-3}	0.237±0.008 (2)
2.32×10^{-3}	0.260[a]	6.06×10^{-3}	0.200±0.004 (3)
5.35×10^{-3}	0.233±0.0001 (2)	1.51×10^{-2}	0.164±0.003 (3)
1.31×10^{-2}	0.165±0.002 (2)	3.71×10^{-2}	0.139±0.007 (4)
2.29×10^{-2}	0.136[a]	8.95×10^{-2}	0.105±0.001 (2)
3.35×10^{-2}	0.102±0.007 (3)		
6.80×10^{-2}	0.086[a]		
7.91×10^{-2}	0.093±0.003 (3)		

a) Measured directly by the FT inversion-recovery technique on the CD_3–CO ^{2}H-signal of Me α-NAc-d_3-Glc.

b) This point was not used in the fitting procedure on account of the high error. All measurements were done in phosphate buffer in D_2O (H_2O for the direct ^{2}H determinations) at 30±1°, pH=6.0 (meter reading), ionic strength 0.08, inhibitor concentration 0.02 mol (0.04 mol for the direct ^{2}H measurement). Errors given are standard deviations. Numbers in parentheses give the number of parallel T_1 measurements.

It can be seen that the relaxation times obtained by the FT method are, in both cases, ca. 20–30% larger than those from the bandshape analysis. This difference is significantly greater than the estimated error (±10%) in either of the two methods. The reason for this discrepancy is not clear at present. We have therefore measured the ^{13}C spin-lattice relaxation times

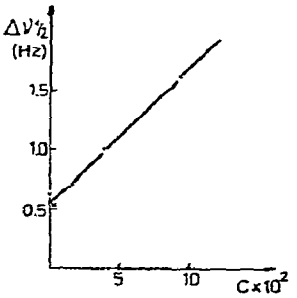

Fig. 3. Proton half-widths ($\Delta\nu_{1/2}$) versus complexed fraction (C) for the acetyl methyl resonance of Me α-NAcGlc.

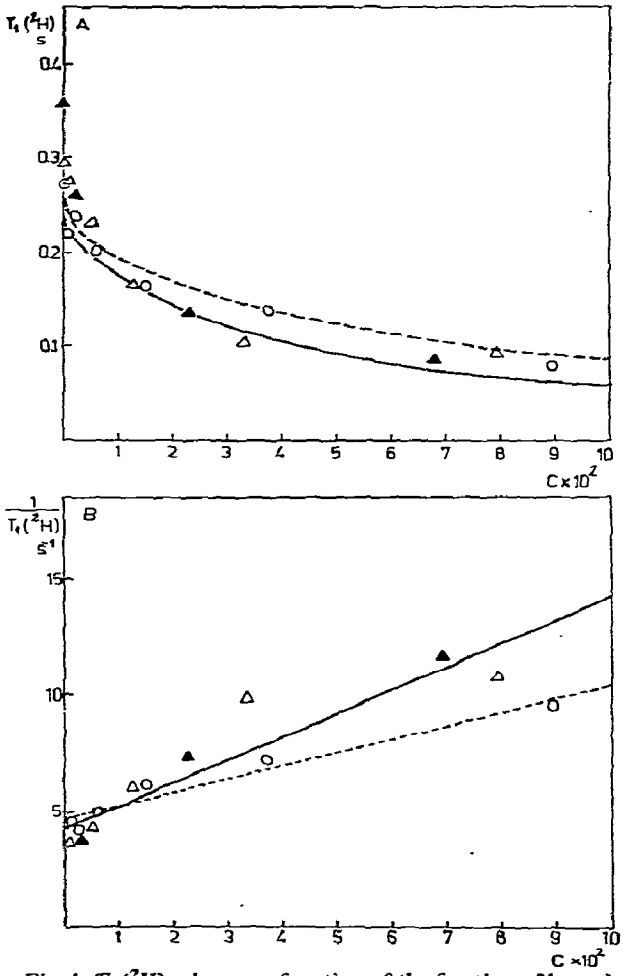

Fig. 4. $T_1(^2H)$ values as a function of the fraction of bound inhibitor for Me α- (triangles) and β-NAcGlc's (circles) measured by the bandshape method (open) on the CH_2D–CO group or by the FT inversion-recovery technique (full) on the CD_3–CO group. Theoretical lines (—— α-anomer, – – – – – β-anomer) were calculated using eqs. (1) (for A) and (3) (for B).

and NOE enhancements for all the carbon atoms in Me α-NAcGlc. The following values were obtained

carbon atoms	C–1	C–2 – C–5	C–6	CH_3–CO	CH_3O
$T_1(^{13}C)$ (s)	0.77	0.77–0.86	0.69	1.81	2.22
NOE	2.95	2.95	2.95	3.00	3.00

Since the NOE for the acetyl methyl carbon shows

Table 3
Data obtained as a result of fitting experimental $T_1(^2H)$ values to eqs. (1) and (3)

	τ_{compl} (s)	$k_2(s^{-1})$	$(T_{1c})^{-1}(s^{-1})$
Lysozyme – Me α-NAcGlc	3.13×10^{-10} (2.42×10^{-10})	3.2×10^9 (4.1×10^9)	134.4 (104.0)
Lysozyme – Me β-NAcGlc	1.79×10^{-10} (1.44×10^{-10})	5.6×10^9 (6.9×10^9)	76.8 (61.9)

Data from eq. (3) are given in parentheses.

that it is relaxed 100% by the dipolar mechanism, we can calculate τ_{free} from eq. (6) [29]

$$T_1(^{13}C)^{-1} = N\hbar^2\gamma_C^2\gamma_H^2 r^{-6}\tau_{free}. \quad (6)$$

Taking r_{CH} = 1.08 Å, we obtain $\tau_{free} = 7.5\times10^{-12}$ s for the N-acetyl methyl carbon atom. From eq. (5) we obtain 7.8×10^{-12} s and 6.5×10^{-12} s for τ_{free} using $T_1(^2H)$ values of 0.294 s (bandshape analysis) and 0.360 s (FT method), respectively, in the case of Me α-NAcGlc. Clearly, neither of these data is accurate enough as to permit a choice between them. We have therefore used a value of 7×10^{-12} s for τ_{free} in both Me α- and β-NAcGlc.

Fig. 4A shows the data of table 2 in graphical form as well as the best fit curves obtained by using eq. (1). Exactly the same calculated curves were obtained with eq. (4) showing that the relevant rotational correlation times (or rotational rate constants, k_1 and k_2) are such that the extreme narrowing approximation can be applied to this case. In the fitting procedure k_3 and k_4 (table 1) were taken to be 1.4×10^5 mol^{-1} s^{-1} and 5.5×10^3 s^{-1} for Me α-NAcGlc and 1.6×10^5 mol^{-1} s^{-1} and 4.5×10^3 s^{-1} for Me β-NAcGlc, respectively. The quadrupole coupling constant, $e^2qQ/\hbar$, was taken to be 170 kHz, a value generally accepted [6,30] for this type of C–D bond. Support for this choice was obtained from the comparison [31–33] of our $T_1(^{13}C)$ and $T_1(^2H)$ data which gave 158 and 175 kHz with $T_1(^2H)$ = 0.360 s and 0.294 s, respectively.

Employing the constants given above, the fit of $T_1(^2H)$ data (table 2) to eq. (1) yielded the values shown in table 3. It is noteworthy that k_2 for Me β-NAcGlc agrees remarkably with the value (4.5×10^9 s^{-1} at 40°) determined [34] by proton T_2 measurements for Me β-NAcGlc complexed with lysozyme

containing Gd (III) ion attached to the active site.

Comparison of k_1 and k_2 with k_3 and k_4 shows that eq. (3) applies equally well since $k_1, k_2 \gg k_3, k_4$. This indeed is the case; $[T_1(^2H)]^{-1}$ shows a linear dependence on the complexed fraction (fig. 4B). Values obtained from the fit to eq. (3) agree within experimental error with those obtained using eq. (1) (table 3).

4.2. *Internal rotation within the EI complex*

$\tau_{compl.}(=1/k_2)$ represents an "effective" correlation time resulting from the overall motions of the EI complex as a unit and local motions of the CH_2D- (or CD_3-) group within this complex. In order to analyze the effective correlation time in terms of overall and internal motions we need to know the rotational correlation time (τ_c) of the lysozyme molecule itself. Dubin et al. [35] reported $\tau_c = 10^{-8}$ s at 20° from light scattering measurements, while application of the Stokes–Einstein equation gave [36] about half of this value. Campbell et al. [37] recently found $\tau_c = 2.8 \times 10^{-9}$ s at 25° from proton NOE measurement. It seems probable that the latter two values are too low since for parvalbumin, a protein similar in size to lysozyme (MW 12 000), $\tau_c = 1.2 \times 10^{-8}$ s has been found both from light scattering [38] and $T_1(^{13}C)$ and ^{13}C NOE measurements [39]. Moreover, from ^{13}C T_1 and NOE data of α-carbon atoms in lysozyme, $\tau_c = 8.5 \times 10^{-9}$ s has been reported [40] at 30°. This is also in agreement with rotational correlation times of $8-10 \times 10^{-9}$ s obtained [41–44] through fluorescence depolarization of lysozyme labelled with a fluorescent dye.

From these data it is evident that τ_c is longer by more than one order of magnitude than the effective correlation time ($\tau_{compl.}$) obtained experimentally for the acetamido methyl group rotations. Such a difference indicates that the methyl group undergoes internal rotation with respect to the overall tumbling of the EI complex. In the crystalline state the sugar molecule is fixed to subsite C by four hydrogen bonds, two of which are directed towards the C=O and NH groups of the acetamido portion of the molecule (cf. section 1). It seems plausible to assume that a similar situation prevails in solution too. Such an arrangement permits the acetamido methyl group to rotate around the CH_3–CO bond. The effect of internal rotation is to decrease the relaxation rate compared to the case when no internal rotation is present. Several theoretical models have been suggested for this type of motion but only two of them will be considered here because they apply outside the extreme narrowing limit as well.

a) Isotropic rotational reorientation combined with internal rotation.

This type of molecular motion has been treated by Woessner [45] in the case of dipole–dipole relaxation. Based on this theory, Andrasko and Forsén [30] derived expressions for the quadrupolar spin-lattice relaxation rates when $\tau_r \ll \tau_c$ (τ_r is the correlation time for internal rotation). Assuming the same conditions to be valid in our case, the correlation time for internal rotation can be expressed as

$$\tau_r = \frac{(T_{1c})^{-1} - 133.1}{1.14 \times 10^{12}}. \qquad (7)$$

To obtain this expression we used $\tau_c = 10^{-8}$ s. With negligibly small τ_r, (7) predicts $\sim 135\ s^{-1}$ as the lower limit for the relaxation rate in the EI complex $[(T_{1c})^{-1}]$.

b) Anisotropic overall reorientation with internal rotation.

This is a more realistic model since the shape of the lysozyme molecule is known to be [35] a prolate ellipsoid of revolution with dimensions of 48 × 26 Å. Woessner et al. [46] have shown that when a group is undergoing internal rotation around an axis the motion of which, in turn, is characterized by two rotational diffusion constants, R_1 and R_2, the spectral densities depend on three diffusion constants (R_1, R_2 and D_1, where D_1 is for the internal rotation) and two angles, θ and α. In our case θ is the angle between the electric field gradient principal axis at the deuteron and the internal rotation axis while angle α is defined by the latter and the R_2 axis of the ellipsoid. The expressions giving the spectral densities are rather complex but they can often be simplified [47]: (i) if the axial ratio of the ellipsoid is known, this gives R_1/R_2; (ii) when the internal rotation is very fast, i.e. $D_1 \gg R_1, R_2$, the second and third terms of eqs. (12) and (15) of ref. [46] vanish and the following equations are obtained for the spectral densities, irrespective of whether the internal rotation is described by a rotational diffusion process or by random jumps between three equivalent positions

$$J_h(\hbar\omega_0) = B_{A1} f_h(\tau_A) + B_{B1} f_h(\tau_B) + B_{C1} f_h(\tau_C),$$

$$h = 1,2, \qquad (8)$$

with

$$\tau_A^{-1} = 6R_2, \quad \tau_B^{-1} = R_1 + 5R_2, \quad \tau_C^{-1} = 4R_1 + 2R_2,$$

$$f_h(\tau_i) = \tau_i/[1 + (h\omega_0\tau_i)^2],$$

$$B_{A1} = \tfrac{1}{8}(1 - 3\cos^2\alpha)^2 (1 - 3\cos^2\theta)^2,$$

$$B_{B1} = \tfrac{3}{8}\sin^2 2\alpha (1 - 3\cos^2\theta)^2,$$

$$B_{C1} = \tfrac{3}{8}\sin^4\alpha (1 - 3\cos^2\theta)^2. \qquad (9)$$

In our case θ may be taken equal to the tetrahedral angle. R_2 is the rotational diffusion constant of the lysozyme molecule about its minor axis. The rotational diffusion constant ($16.7 \times 10^6\ s^{-1}$) obtained from light scattering measurements is associated just with this motion [35]. From the axial ratio, 48/26 = 1.846, we get $16.7 \times 1.846 \times 10^6\ s^{-1} = 30.8 \times 10^6\ s^{-1}$ for R_1. This leaves us with one unknown, α, in eqs. (8)–(9). Since α cannot be determined from our experiments we have calculated

$$J_1(\omega_0) + 4J_2(2\omega_0) = \tau_{\text{compl.}}$$

for a series of α values ranging from 0° to 180°. Using the constants (R_1, R_2 and θ) given above we got the following diagram (fig. 5). The corresponding relaxation rates can be readily calculated from eq. (10) [15],

$$(T_{1c})^{-1} = \frac{3}{80}\left(\frac{e^2qQ}{\hbar}\right)^2 [J_1(\omega_0) + 4J_2(2\omega_0)]. \qquad (10)$$

Assuming, as before, the quadrupole coupling constant equal to 170 kHz, the relaxation rates corresponding to the extrema of the curve on fig. 5 are,

$$(T_{1c})_0^{-1} = \frac{3}{80} 4\pi^2 (1.7 \times 10^5)^2 \times 3.14 \times 10^{-9} \approx 135\ s^{-1},$$

similarly,

$$(T_{1c})_{50}^{-1} = 309\ s^{-1}, \qquad (T_{1c})_{90}^{-1} = 223\ s^{-1}.$$

The limiting values of the calculated relaxation rates in both models are determined by the rotational correlation time (τ_c) of lysozyme. We have seen that realistic values of τ_c vary between $8–12 \times 10^{-9}$ s which corresponds to a change from $140\ s^{-1}$ to $124\ s^{-1}$ in $(T_{1c})^{-1}$ for the isotropic case. On the other hand, experimental relaxation rates (table 3) are influenced, in addition to the experimental errors of the relaxation time measurements, by the inaccuracy of the quadrupole coupling constant (estimated error ± 10%) and errors in the extrapolation procedure itself.

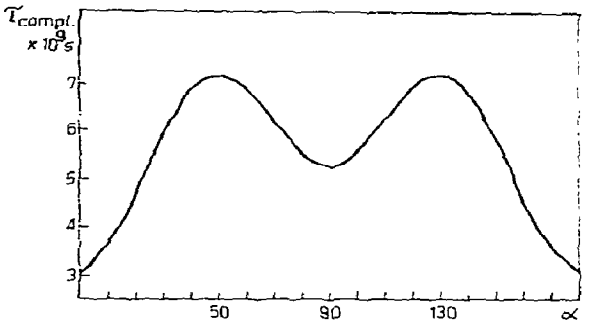

Fig. 5. Variation of $\tau_{compl.}$ as a function of the angle α between the internal rotation axis and the major ellipsoidal axis of the lysozyme molecule.

Taking into account these uncertainties, the estimated relaxation rates, using either the isotropic model [eq. (7)] or the anisotropic approximation with $\alpha \sim 0°$, agree fairly well with $(T_{1c})^{-1}$ measured in the Me α-NAcGlc complex (table 3). This result suggests that, within the frame of the anisotropic model, (i) the internal rotation of the acetamido methyl is fast ($D_1 \gg R_1, R_2$) in this complex and, (ii) the rotation axis is nearly parallel ($\alpha \sim 0°$) with the major ellipsoidal axis of the lysozyme molecule.

In contrast to the case above, for the Me β-NAcGlc complex consistently smaller relaxation rates (table 3) were obtained than the minimum values calculated with the assumption of fast internal rotation in either the isotropic [$(T_{1c})^{-1} = 131\ s^{-1}$] or the anisotropic [$(T_{1c})^{-1} = 135\ s^{-1}$] models. Since the difference between the extrapolated relaxation rates in the two complexes could hardly be attributed to any systematic experimental errors, the low value of $(T_{1c})^{-1}$ in the Me β-NAcGlc complex could be interpreted by assuming that, in addition to the rotation around the CH_3–CO bond, there is another degree of rotational freedom for the acetamido methyl group. It seems plausible to assume that the structures of the glycoside complexes are closely analogous to those of the free monosaccharides (at least so far as the binding of the

acetamido side chain is concerned) as determined from X-ray crystallography [1,2]. If this is the case, it is difficult to imagine an additional internal rotation (about an axis else than the CH_3–CO bond) in an acetamido group anchored to the enzyme by two hydrogen bonds. At the present stage of our work we cannot offer a simple explanation for this discrepancy and, clearly, more experimental work is needed to clarify this point.

5. Conclusion

Measurement of the deuteron spin-lattice relaxation times of specifically labelled inhibitor molecules, participating in an association equilibrium with enzymes, offers a convenient approach for studying molecular motions of the inhibitor within the EI complex.

Comparison of the relaxation rates of deuterons, built into the acetamido methyl groups of methyl N-acetyl glucosaminide inhibitors, with the results of model calculations shows that in the Me α-NAcGlc – lysozyme complex the acetamido methyl group is likely to undergo fast internal rotation about an axis which is nearly parallel with the major ellipsoidal axis of the lysozyme molecule.

The smaller relaxation rate found in Me β-NAcGlc complex is tentatively attributed to a second rotation within the acetamido group in addition to the CH_3 – CO internal rotation. Such a model seems to be at variance with X-ray crystallographic results obtained with α- and β-NAcGlc – lysozyme complexes.

Acknowledgement

Thanks are due to Professors R. Bognár and P. Nánási (Debrecen) for their interest. L.Sz. is deeply indebted to Professor J.-M. Lehn who initiated this author to the field of molecular dynamics. We express our gratitude to dr. J.-P. Behr (Strasbourg) for a band-shape program and for carrying out some preliminary calculations and to dr. T. Drakenberg (Lund) who sent his results on liver alcohol dehydrogenase prior to publication. Mr. A. Löki (Debrecen) is thanked for drawing the diagrams and for his help in the experimental work.

References

[1] D.C. Phillips, Sci. Amer. 215/5 (1966) 78; Proc. Nat. Acad. Sci. U.S. 57 (1967) 484.
[2] C.C.F. Blake, L.N. Johnson, G.A. Mair, A.C.T. North, D.C. Phillips and V.R. Sarma, Proc. Roy. Soc. (London) 167B (1967) 378.
[3] L.E.H. Smith, L.H. Mohr and M.A. Raftery, J. Am. Chem. Soc. 95 (1973) 7497.
[4] R.F. Atkinson and T.C. Bruice, J. Am. Chem. Soc. 96 (1974) 819.
[5] G.M. Loudon, C.K. Smith and S.E. Zimmerman, J. Am. Chem. Soc. 96 (1974) 465;
see, however, M. Levitt, in: Peptides, polypeptydes and proteins, Proc. Rehovot Symp., eds. E.R. Blout, F.A. Bovey and M. Goodman (Wiley, New York, 1974) p. 99.
[6] C. Brévard, J.-P. Kintzinger and J.-M. Lehn, Tetrahedron 28 (1972) 2429, and references therein.
[7] D.M. Chipman and N. Sharon, Science 165 (1969) 454.
[8] T. Imoto, L.N. Johnson, A.C.T. North, D.C. Phillips and J.A. Rupley, in: The enzymes, ed. P. Boyer (3rd Ed. Academic Press, New York, 1972) pp. 665–868.
[9] M.A. Raftery, F.W. Dahlquist, S.I. Chan and S.M. Parsons, J. Biol. Chem. 243 (1968) 4175.
[10] B.D. Sykes, Biochemistry 8 (1969) 1110.
[11] J. Verhoeven and R. Schwyzer, Helv. Chim. Acta 55 (1972) 2572.
[12] J.A. Ruply, L. Butler, M. Gerring, F.J. Hartdegen and R. Pecoraro, Proc. Nat. Acad. Sci. U.S. 57 (1967) 1088.
[13] H. Saitô, L.C. Leitch and I.C.P. Smith, J. Am. Chem. Soc. 96 (1974) 256.
[14] J.-P. Kintzinger, J.-M. Lehn and R.L. Williams, Mol. Phys. 17 (1969) 135.
[15] A. Abragam, The principles of nuclear magnetism (Clarendon Press, Oxford, 1961).
[16] R.L. Vold, J.S. Waugh, M.P. Klein and D.E. Phelps, J. Chem. Phys. 48 (1968) 3831.
[17] J.E. Anderson, Ber. Bunsenges. Phys. Chem. 75 (1971) 294.
[18] J.E. Anderson and P.A. Fryer, J. Chem. Phys. 50 (1969) 3784.
[19] F.I. Andersen, Nature 173 (1954) 541.
[20] D. Horton, in: Methods in carbohydrate chemistry, vol. 6 eds. R.L. Whistler and J.N. BeMiller (Academic Press, New York, 1972) p. 282.
[21] F. Zilliken, C.S. Rose, G.A. Braun and P. György, Arch. Biochem. Biophys. 54 (1955) 392.
[22] J. Conchie and G.A. Levvy, in: Methods in carbohydrate chemistry, vol. 2, eds. R.L. Whistler and M.L. Wolfrom (Academic Press, New York, 1963) p. 334.
[23] D. Shugar, Biochem. Biophys. Acta 8 (1952) 302.
[24] R.C. Davies, A. Neuberger and B.M. Wilson, Biochim. Biophys. Acta 178 (1969) 294.
[25] D.L. Van der Hart, J. Chem. Phys. 60 (1974) 1858.
[26] J.-P. Kintzinger, Thesis (Strasbourg, 1970).
[27] C. Brévard and J.-M. Lehn, J. Am. Chem. Soc. 92 (1970) 4987.

[28] F.W. Dahlqist and M.A. Raftery, Biochemistry 7 (1968) 3269.
[29] J.R. Lyerla and D.M. Grant, in: MTP Internat. Rev. Sci. Phys. Chem., Series I, vol. 4 eds. A.D. Buckingham and C.A. McDovell (Butterworths, London, 1972) p. 155.
[30] J. Andrasko and S. Forsén, Chem. Scripta 6 (1974) 163.
[31] L.M. Jackman, E.S. Greenberg, N.M. Szeverényi and G.K. Schnorr, J.C.S. Chem. Comm. (1974) 141.
[32] J.-P. Kintzinger and J.-M. Lehn, J. Am. Chem. Soc. 96 (1974) 3313.
[33] H. Saitô, H.H. Mantsch and I.C.P. Smith, J. Am. Chem. Soc. 95 (1973) 8453.
[34] K.G. Morallee, E. Nieboer, F.J.C. Rossotti, R.J.P. Williams and A.V. Xavier, Chem. Comm. (1970) 1132.
[35] S.B. Dubin, N.A. Clark and G.B. Benedek, J. Chem. Phys. 54 (1971) 5158.
[36] R.A. Dwek, in: N.M.R. in biochemistry (Clarendon Press, Oxford, 1973) p. 303.
[37] I.D. Campbell, C.M. Dobson and R.J.P. Williams, J.C.S. Chem. Comm. (1974) 888.
[38] D.R. Bauer, S.J. Opella, D.J. Nelson and R. Pecora, J. Am. Chem. Soc. 97 (1975) 2850.
[39] S.J. Opella, D.J. Nelson and O. Jardetzky, J. Am. Chem. Soc. 96 (1974) 7175.
[40] P. Cozzone, S.J. Opella, O. Jardetzky, O. Berthou and P. Jollès, Proc. Nat. Acad. Sci. U.S. 72 (1975) 2095.
[41] R. Irwin and J.E. Churchic, J. Biol. Chem. 246 (1971) 5329.
[42] A.B. Rawich, Arch. Biochem. Biophys. 151 (1972) 22.
[43] R.F. Chen, Anal. Lett. 7 (1974) 65.
[44] L.H. Tang, Y. Kubota and R.F. Steiner, Biophys. Chem. 4 (1976) 203.
[45] D.E. Woessner, J. Chem. Phys. 36 (1962) 1.
[46] D.E. Woessner, B.S. Snowden and G.H. Meyer, J. Chem. Phys. 50 (1969) 719.
[47] T. Drakenberg, J. Magn. Res. 15 (1974) 354.